# NLO Lecture 21: Terahertz Generation and Applications

**11.2 Optical rectification (Continued)**

**11.2.1 Optical rectification with tilted-pulse-fronts**

**11.2.2 Optical rectification by Quasi-Phase Matching (QPM)**

# Tilted pulse front technique

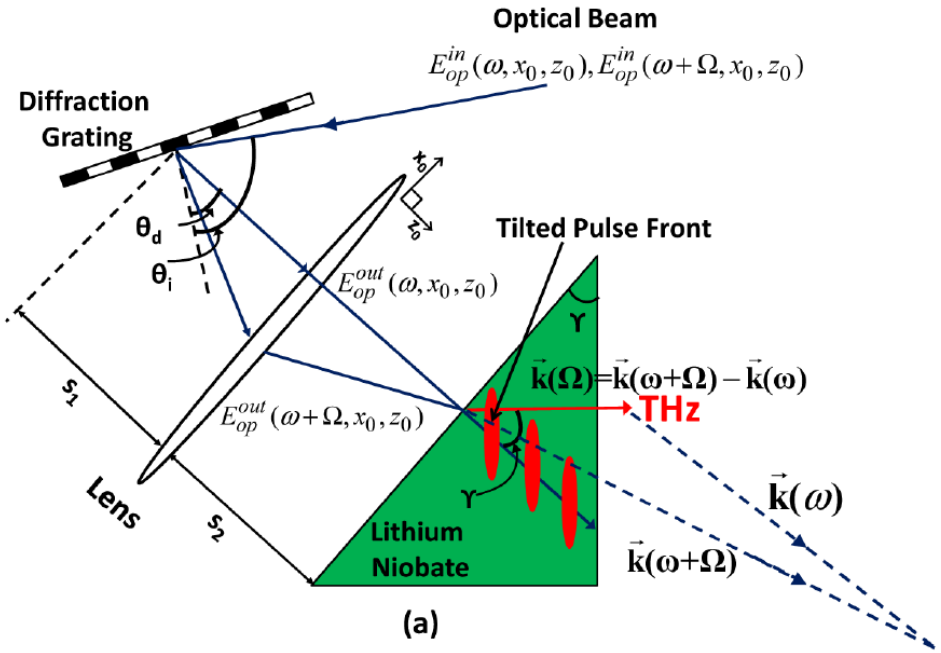


(a)

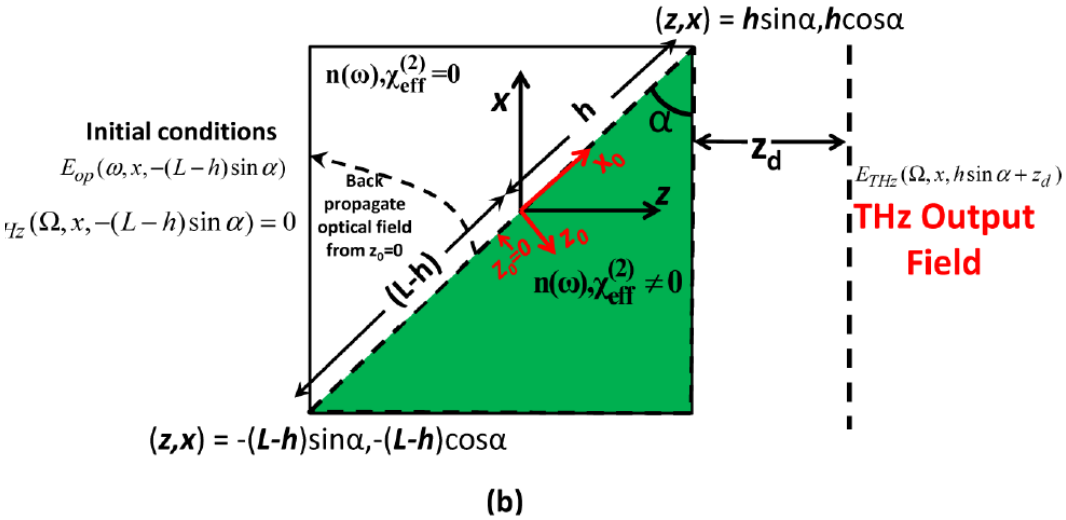


(b)

# Non-collinear phase matching

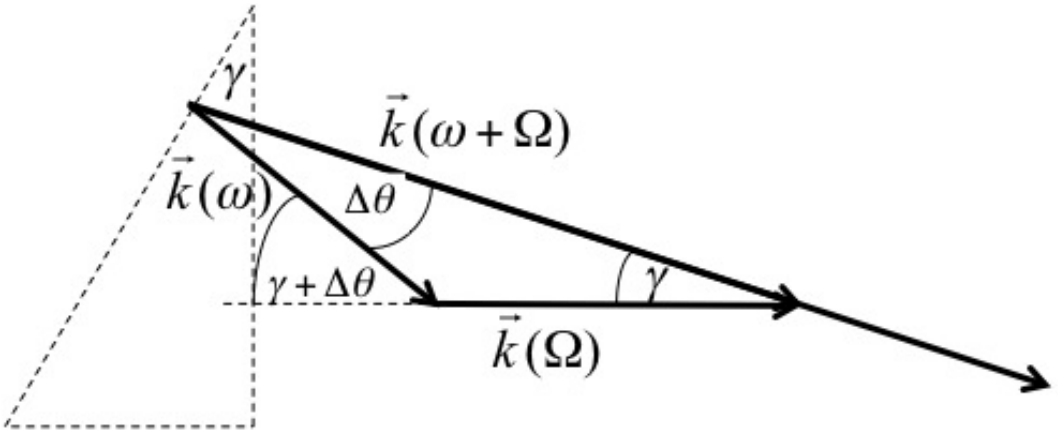


**Figure 11.6:** Noncollinear phase-matching condition for pulse-front-tilted optical rectification.

**z - component**

$$\begin{aligned}\Delta k_z(\omega) &= \cos\gamma\ k(\omega+\Omega) - \cos(\gamma+\theta(\omega))\ k(\omega) - k_{THz}(\Omega) \\ &= \cos\gamma\ \frac{\partial k_{opt}(\omega)}{\partial\omega}\Omega + \sin\gamma\left(-\frac{\partial\theta}{\partial\omega}\right)\Omega\ k(\omega) - k_{THz}(\Omega) = 0,\end{aligned}$$

**y - component**

$$\begin{aligned}\Delta k_y(\omega) &= \sin\gamma\ k(\omega+\Omega) - \sin(\gamma+\theta(\omega))\ k(\omega) \\ &= \sin\gamma\frac{\partial k_{opt}(\omega)}{\partial\omega}\Omega - \cos\gamma\frac{\partial\theta}{\partial\omega}\Omega\ k(\omega) \\ &= \sin\gamma\frac{\partial k_{opt}(\omega)}{\partial\omega}\Omega - \cos\gamma\left(-\frac{\partial\theta}{\partial\omega}\right)\Omega\ k(\omega) = 0.\end{aligned}$$

**Tilt angle**

$$\begin{aligned} \frac{\partial k_{opt}(\omega)}{\partial \omega}\Omega - \cos\gamma k_{THz}(\Omega) &= 0 \\ \frac{1}{v_{g,opt}} - \frac{1}{v_{p,THz}}\cos\gamma &= 0 \\ n_{g,opt} &= n_{p,THz}\ \cos\gamma, \end{aligned}$$

**Necessary angular spread**

$$\frac{\partial\theta}{\partial\omega} = -\tan\gamma\frac{v_{p,opt}}{\omega\ v_{g,opt}} = -\tan\gamma\frac{n_{g,opt}}{\omega\ n_{p,opt}}.$$

**1D – spatial Model**

$$\begin{aligned} k(\omega) &= \frac{1}{\cos\gamma}\frac{\omega\ n(\omega)}{c} + \frac{(\omega-\omega_0)^2}{2}k''_{AD} \\ k''_{AD} &= \frac{-n^2_{g,opt}(\omega_0)}{\omega_0\ c\ (\omega_0)}\tan^2\gamma. \end{aligned}$$

# 1D - Model

$$\frac{d\hat{E}_{THz}(\Omega,z)}{dz} = -\frac{\alpha_{THz}(\Omega)}{2}\hat{E}_{THz}(\Omega,z) - j\frac{\Omega\ d_{eff}}{c\ n_{p,THz}}\int_0^\infty \hat{E}_{opt}(\omega+\Omega,z)\ \hat{E}_{opt}(\omega,z)^*\ e^{j\Delta k(\omega)z}d\omega\ . \tag{11.13}$$

which also includes the THz absorption. For the optical field, we obtain

$$\begin{aligned}\frac{d\hat{E}_{opt}(\omega,z)}{dz} = & -\frac{\alpha_{opt}(\Omega)}{2}\hat{E}_{opt}(\omega,z) \\ & -j\frac{\omega\ d_{eff}}{c\ n_{p,opt}}\int_0^\infty \hat{E}_{opt}(\omega+\Omega,z)\ \hat{E}_{THz}(\Omega,z)^*\ d\Omega e^{-j\Delta k(\omega)z} \\ & -j\frac{\omega\ d_{eff}}{c\ n_{p,opt}}\int_0^\infty \hat{E}_{opt}(\omega-\Omega,z)\ \hat{E}_{THz}(\Omega,z)\ e^{-j\Delta k(\omega)z}d\Omega \\ & +\mathcal{F}\left[j\frac{\varepsilon_0\omega_0\ n_{p,opt}^2\ n_2 d_{eff}}{2}\left|E_{opt}(t,z)\right|^2\ E_{opt}(t,z)\right] \\ & +\mathcal{F}\left[j\frac{\varepsilon_0\omega_0\ n_{p,opt}^2\ n_2 d_{eff}}{2}\left[\left|E_{opt}(t-t',z)\right|^2\otimes h_r(t')\right]\ E_{opt}(t,z)\right],\end{aligned} \tag{11.14}$$

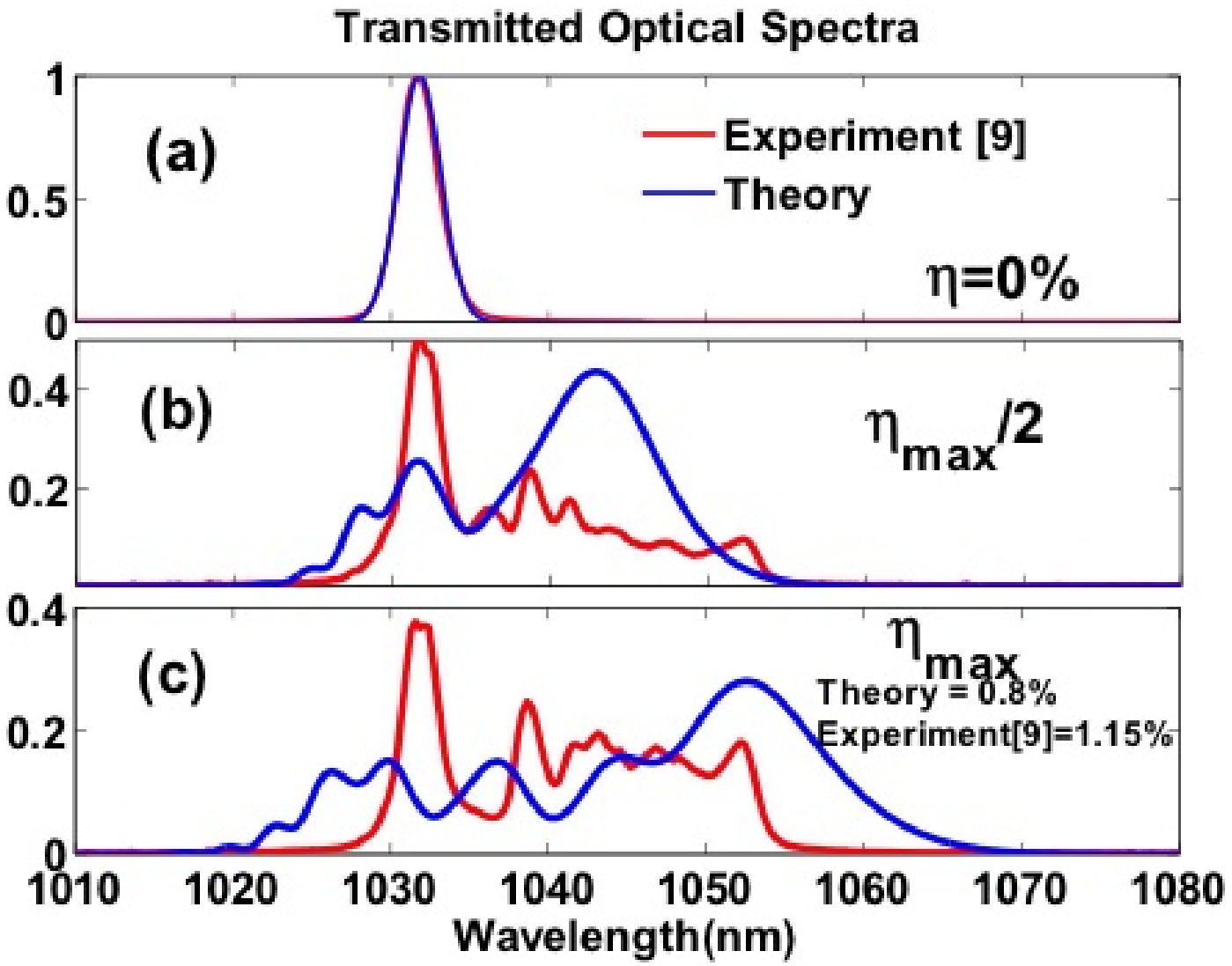


Figure 11.7: Comparison of experimental and simulated optical spectra for different amounts of generated THz.

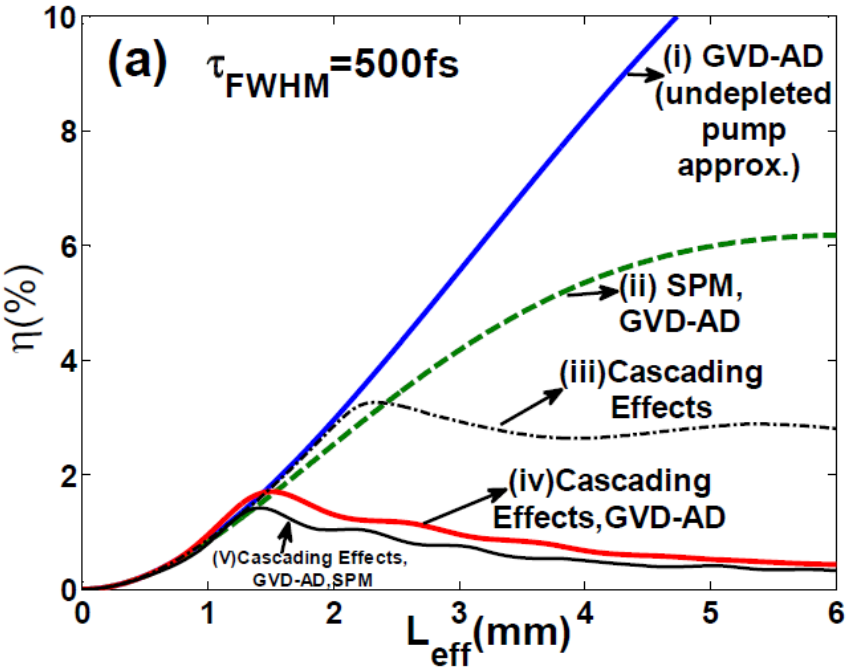


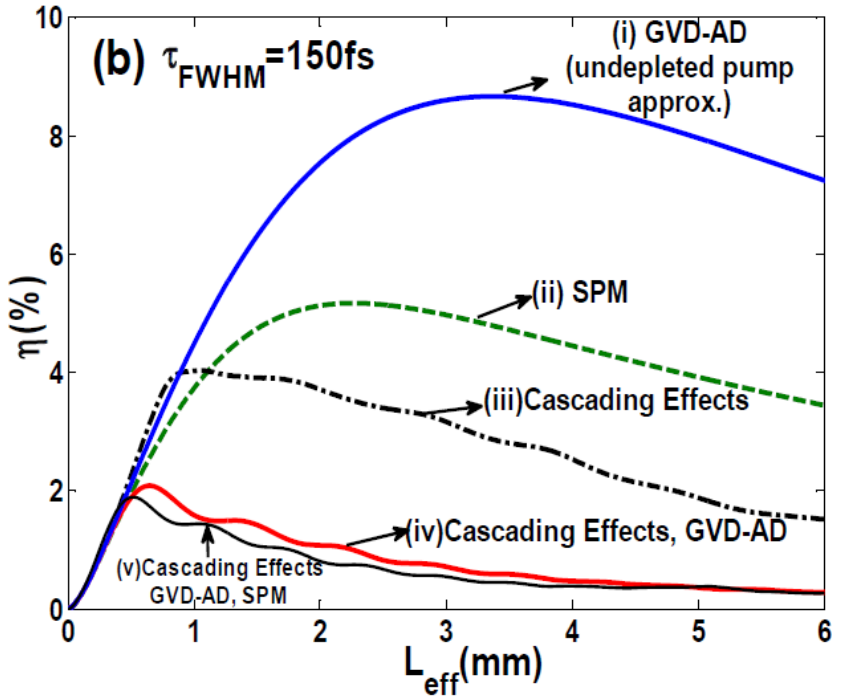


Figure 11.8: Conversion efficiencies as a function of effective length are calculated by switching on/off various effects. Material dispersion and absorption are considered for all cases. The pump fluence is 20 mJ/cm2, for a crystal temperature of 100 K. (a) Gaussian pulses with 500-fs FWHM pulse width with peak intensity of 40 GW/cm2 are used. Cascading effects together with GVD-AD leads to the lowest conversion efficiencies. The drop in conversion efficiency is attributed to the enhancement of phase mismatch caused by dispersion due to the large spectral broadening caused by THz generation (See Figs. 11.7(b)-(c)). However, since group velocity dispersion due to angular dispersion (GVD-AD) is more significant than GVD due to material dispersion at optical frequencies in lithium niobate, cascading effects in conjunc- tion with GVD-AD is the strongest limitation to THz generation. SPM effects are much less detrimental since they cause relatively small broadening of the optical pump spectrum (see 11.7 (a)). (b) Cascading effects along with GVD-AD are most detrimental even for a 150-fs Gaussian pulse with 3× larger peak intensity. [19]

# 2D - Simulation

(a) SPM, GVD-AD, material dispersion, absorption

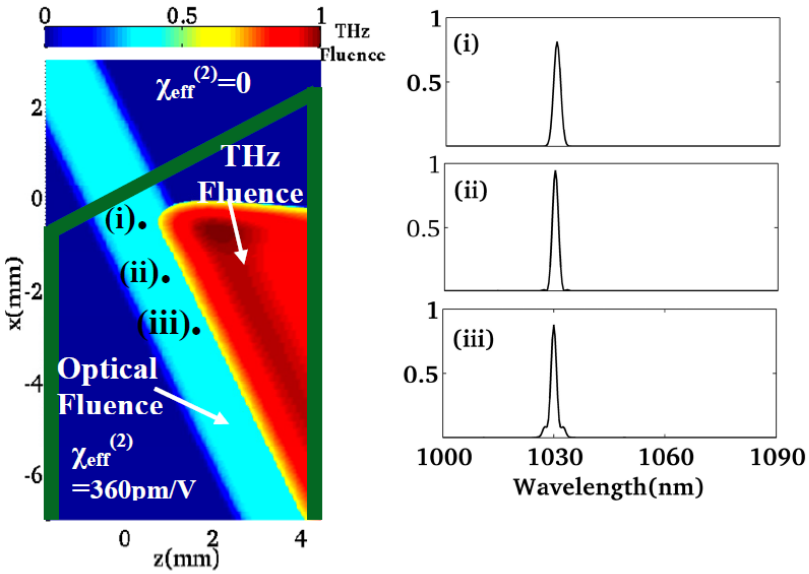


(b) Cascading Effects, GVD-AD, material dispersion, absorption

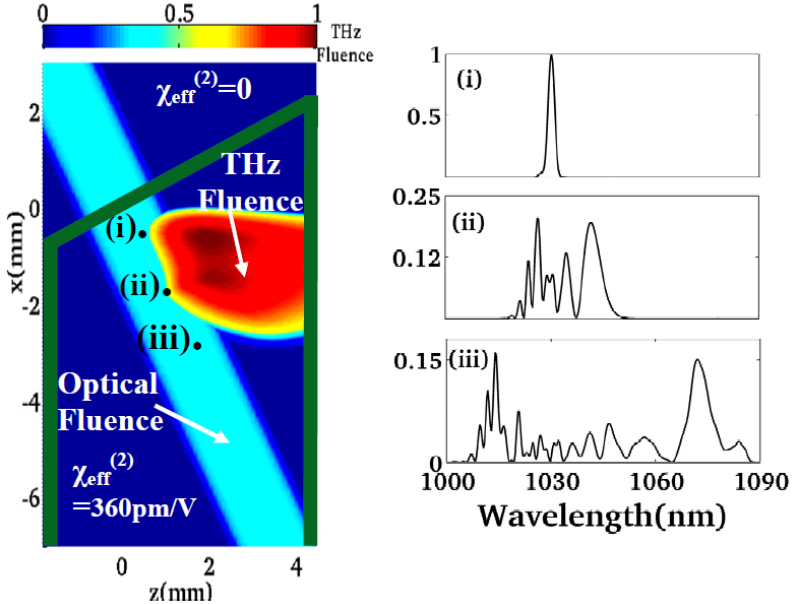

# THz Generation results

~1% optical to THz conversion

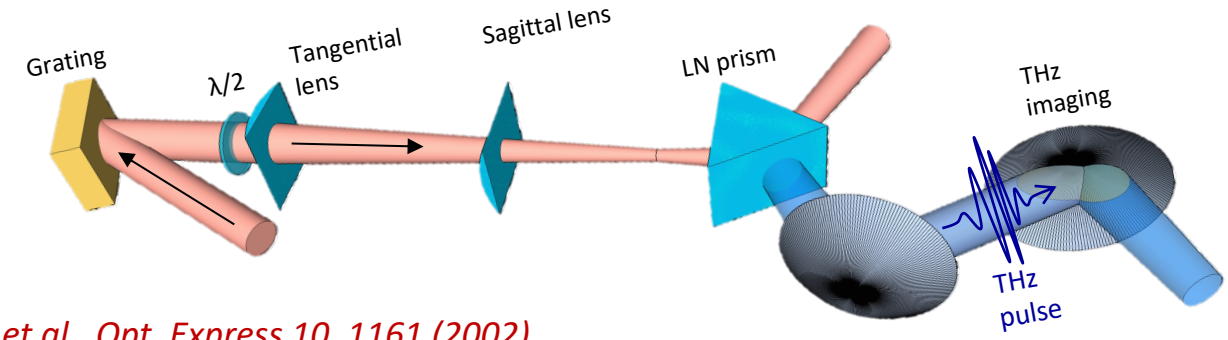


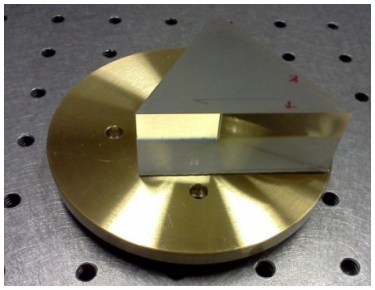

LN prism

*J. Hebling et al., Opt. Express 10, 1161 (2002)*
*J. A. Fülöp et al., Opt. Express 19, 15090 (2011)*
*S. W. Huang et al Opt. Lett. 38(5), 796-798 (2013)*
*X. Wu et al., Opt. Express 24, 21059 (2016)*

Single-cylce THz generation:

$E_{THz}$ ~ 200 μJ

$f_{THz}$ ~ 280 GHz

$\Delta_{FWHM}$ ~ 3.3 ps

IR laser: 40 mJ, 1020 nm, 1ps

0.5 % efficiency

Measured THz mode

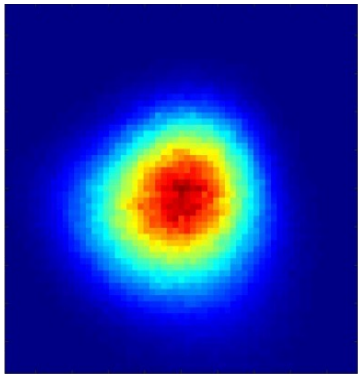

**Measured THz Waveform**

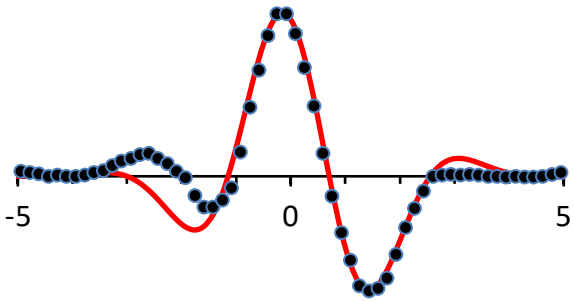


Delay [ps]

# 1.4 mJ THz Generation Results from Ti:Sapphire Laser

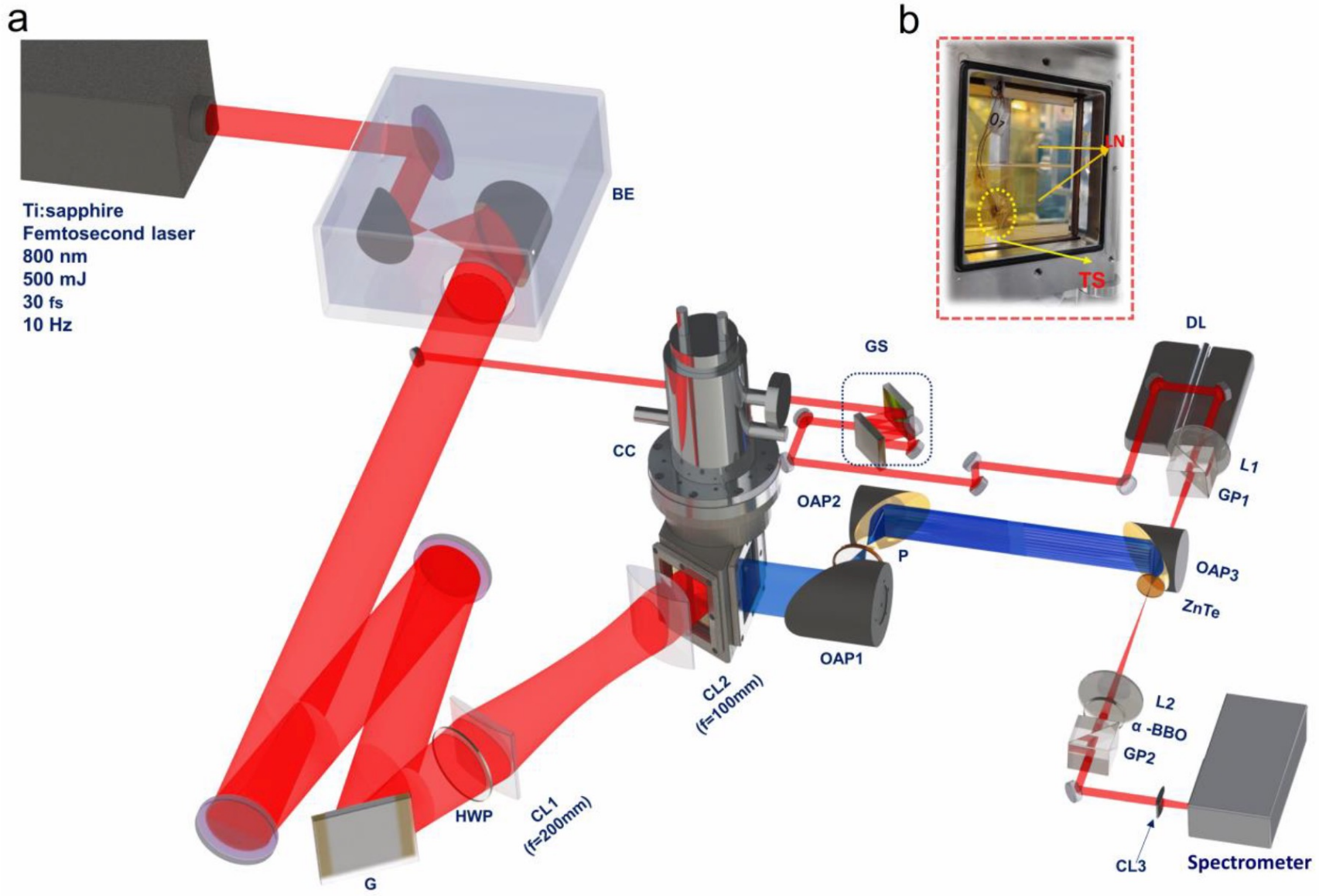


B. Zhang, …. Xiaojun Wu, ….., 1.4-mJ High Energy Terahertz Radiation from Lithium Niobate, LPR 15 (2021), doi: 10.1002/lpor.202000295.

# 1.4 mJ THz Generation Results from Ti:Sapphire Laser

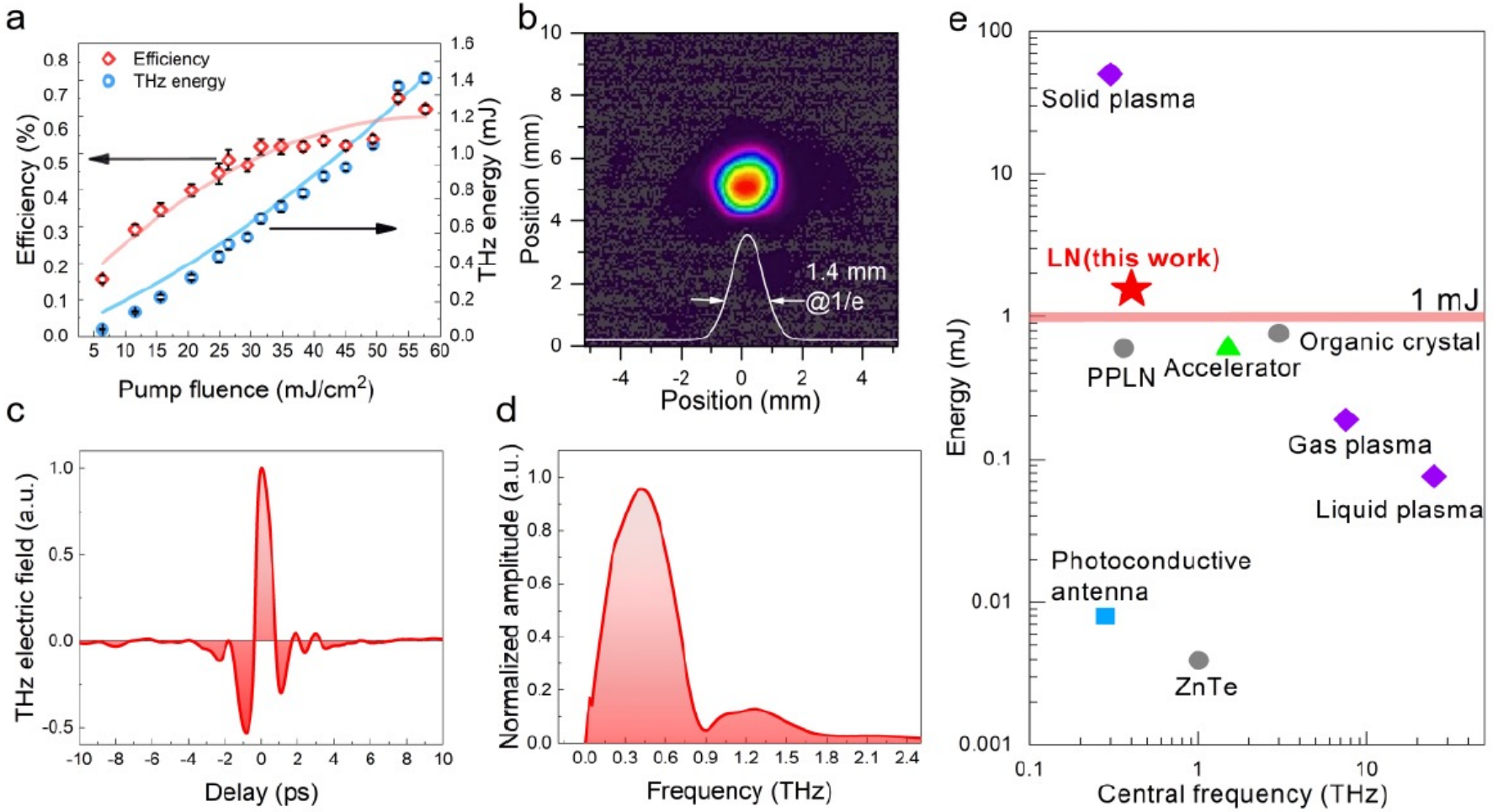


B. Zhang, …. Xiaojun Wu, ….., 1.4-mJ High Energy Terahertz Radiation from Lithium Niobate, LPR 15 (2021), doi: 10.1002/lpor.202000295.

# 11.2.2 Optical rectification by Quasi-Phase Matching (QPM)

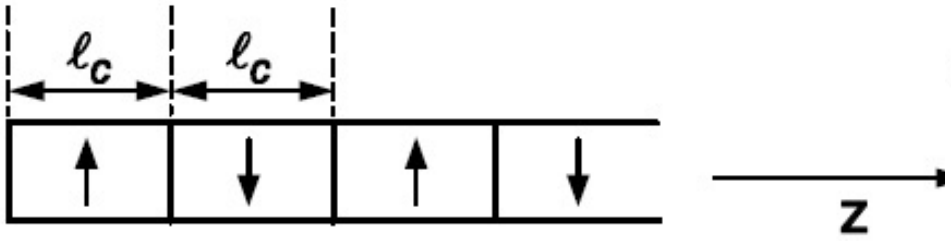


Periodically poled crystal

$$d_{eff}(z) = \sum_{m=-\infty}^{+\infty} d_m e^{jm\kappa z}$$

$$\begin{aligned}
\Delta k &= \left.\frac{\partial k_{opt}(\omega)}{\partial \omega}\right|_{\omega_0} \Omega - k_{THz}(\Omega) + m\frac{2\pi}{\Lambda} = \left(\frac{1}{v_{g,opt}} - \frac{1}{v_{p,THz}}\right)\Omega + m\frac{2\pi}{\Lambda} \\
&= \left(\frac{n_{g,opt} - n_{p,THz}}{c}\right)\Omega + m\frac{2\pi}{\Lambda} = 0 \\
\rightarrow \quad & \Lambda = m\frac{\lambda_{THz}}{n_{p,THz} - n_{g,opt}}.
\end{aligned}$$

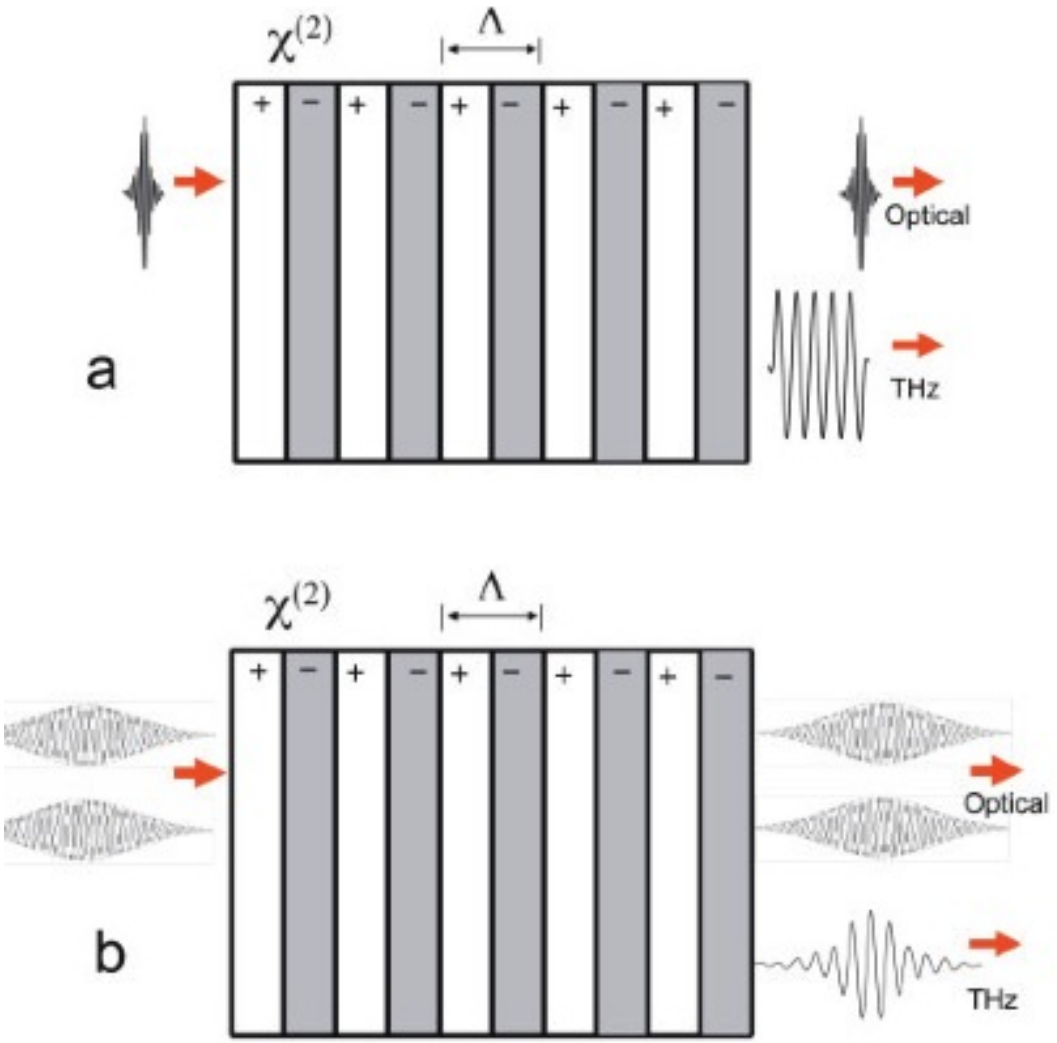


**Figure 11.10**: Schematic illustration of collinear THz-wave generation in a nonlin- ear crystal with periodically inverted sign of χ(2). (a) Optical rectification with femtosecond pulses, (b) difference-frequency generation with two picosecond pulses (Ω = ω3 − ω2) [10].

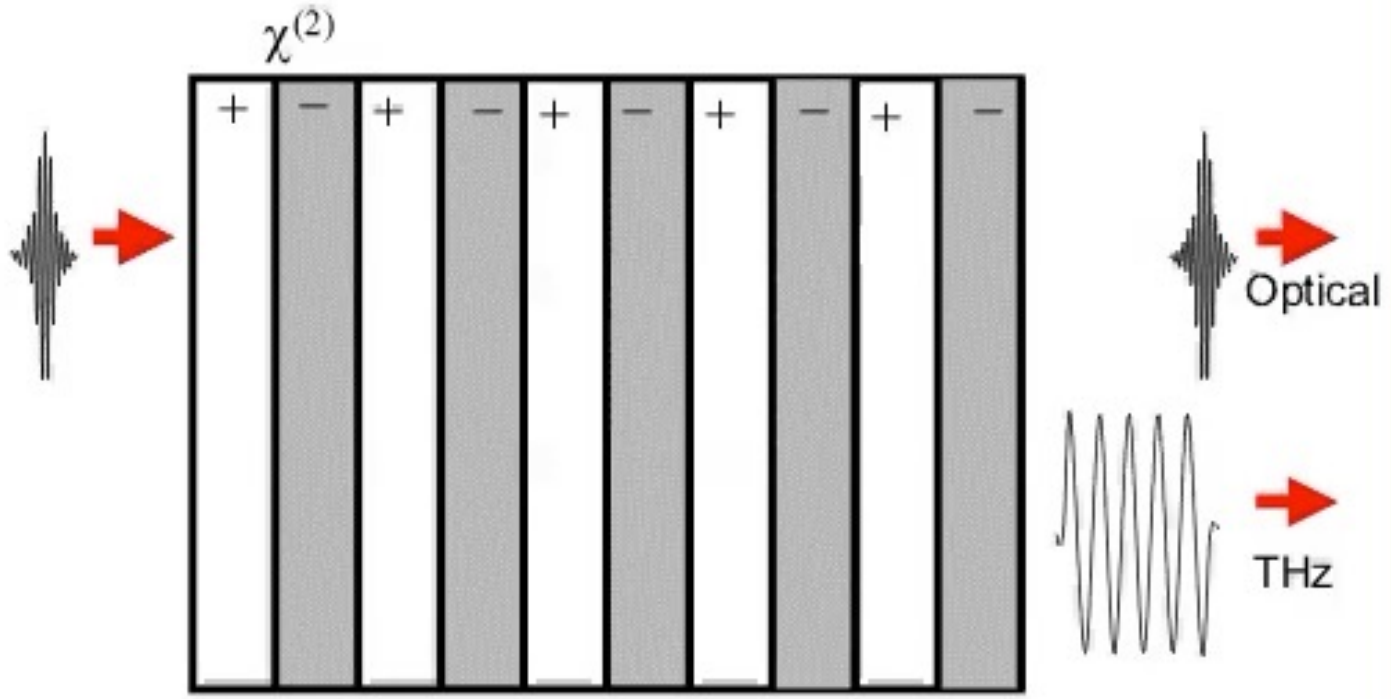
$\chi^{(2)}$
+
−
+
−
+
−
+
−
+
−
Optical
THz

## Plane-wave analysis of optical-to-THz conversion in QPM crystals with ultrashort pulses

$$E_{opt}(t) = Re\{E_0\ e^{-t^2/\tau^2}\ e^{j\omega_0 t}\} = \frac{1}{2}\{E_0\ e^{-t^2/\tau^2}\ e^{j\omega_0 t} + c.c.\},$$

$$\hat{E}_{opt}(\omega) = \frac{E_o \tau}{2\sqrt{\pi}} \exp\left(-\frac{\tau^2\omega^2}{4}\right)$$

$$\begin{aligned}\frac{d\hat{E}_{THz}(\Omega, z)}{dz} &= -j\frac{\Omega\ d_{eff}^{QPM}}{c\ n_{p,THz}} \frac{E_o^2\tau^2}{4\pi} \int_{-\infty}^{+\infty} \exp\left(-\frac{\tau^2(\omega+\Omega)^2}{4}\right) \exp\left(-\frac{\tau^2\omega^2}{4}\right) d\omega \\ &= -j\frac{\Omega\ d_{eff}^{QPM}}{c\ n_{p,THz}} \frac{E_o^2\tau}{2\sqrt{2\pi}} \exp\left(-\frac{\tau^2\Omega^2}{8}\right)\ e^{j\Delta k(\Omega)z}. \qquad (11.23)\end{aligned}$$

$$\left|\hat{E}_{THz}(\Omega, z)\right|^2 = \frac{\Omega^2\ d_{eff}^{QPM,2}}{c^2\ n_{p,THz}^2} \frac{E_o^4\tau^2}{8\pi} \exp\left(-\frac{\tau^2\Omega^2}{4}\right)\ L^2\mathrm{sinc}^2\left(\frac{\Delta k(\Omega)L}{2}\right) \qquad (11.24)$$

$$\text{with } \Delta k(\Omega) = \Delta k = \frac{n_{g,opt} - n_{p,THz}}{c} + m\frac{2\pi}{\Lambda} \qquad (11.25)$$

$$d_{eff}^{QPM} = \frac{2}{\pi} d_{eff}$$

# Optical to THz conversion effficiency

$$\eta_{THz}^{PW} = \frac{\text{Fluence THz}}{\text{Fluence (pump)}}$$

$$F_{pump} = \frac{c\varepsilon_0 n_{p,opt}}{2}\int_{-\infty}^{+\infty}\left|E_{opt}\left(t,0\right)\right|^2 dt = \sqrt{\frac{\pi}{2}}\frac{c\varepsilon_0 n_{p,opt}}{2}E_o^2\tau$$

and THz fluence

$$F_{THz} = \frac{c\varepsilon_0 n_{p,THz}}{2}\int_{-\infty}^{+\infty}\left|E_{THz}\left(t,L\right)\right|^2 dt = \frac{c\varepsilon_0 n_{p,THz}}{2}2\pi\int_{-\infty}^{+\infty}\left|\hat{E}_{THz}\left(\Omega,z\right)\right|^2 d\Omega \quad (11.28)$$

where we used Parceval's theorem

$$\int_{-\infty}^{+\infty}\left|f(t)\right|^2 dt = 2\pi\int_{-\infty}^{+\infty}\left|\hat{f}\left(\Omega\right)\right|^2 d\Omega. \quad (11.29)$$

Thus, we obtain

$$N = \frac{L}{\Lambda}$$

$$\eta_{THz}^{PW} = \frac{\Omega^2\ d_{eff}^{QPM,2}E_o^2\tau}{2\sqrt{2\pi}c^2\ n_{p,opt}n_{p,THz}}L^2\int_0^{+\infty}\exp\left(-\frac{\tau^2\Omega^2}{4}\right)\ \text{sinc}^2\left(\frac{\pi}{2}\frac{\Omega-\Omega_0}{\Delta\Omega}\right)d\Omega, \quad (11.30)$$

$$\text{with } \Omega_0 = \frac{2\pi\ c}{\Lambda\left(n_{g,opt}-n_{p,THz}\right)} \text{ and } \Delta\Omega = \frac{2\pi\ c}{L\left(n_{g,opt}-n_{p,THz}\right)} = \frac{\Lambda}{L}\Omega_0 \quad (11.31)$$

$$\eta_{THz}^{PW,sp} = \frac{\Omega^2 \; d_{eff}^{QPM,2} E_o^2 c}{2\sqrt{2\pi} c^2 \; n_{p,opt} n_{p,THz}} \; L^2 g_1(\Omega_0) \; 2 \; \Delta\Omega =$$

$$= \frac{\Omega^2 \; d_{eff}^{QPM,2} E_o^2 \tau}{c \; n_{p,opt} n_{p,THz}} \; \frac{\sqrt{2\pi}}{(n_{g,opt} - n_{p,THz})} \; L \; g(\Omega_0)$$

$$= \frac{2\Omega^2 \; d_{eff}^{QPM,2} L}{\varepsilon_0 \; c^2 \; n_{p,opt}^2 n_{p,THz} \, (n_{g,opt} - n_{p,THz})} \; g_1(\Omega_0) \; F_{pump} \quad (11.32)$$

$$\text{with } g_1(\Omega_0) = \exp\left(-\frac{\tau^2 \Omega_0^2}{4}\right) = \exp\left(-\left(\pi f_{THz} \tau\right)^2\right) \text{ and} \quad (11.33)$$

$$2 \; \Delta\Omega = \int_{-\infty}^{+\infty} \mathrm{sinc}^2\left(\frac{\pi}{2} \frac{\Omega - \Omega_0}{\Delta\Omega}\right) \, d\Omega \quad (11.34)$$

# Influence of optical bandwidth

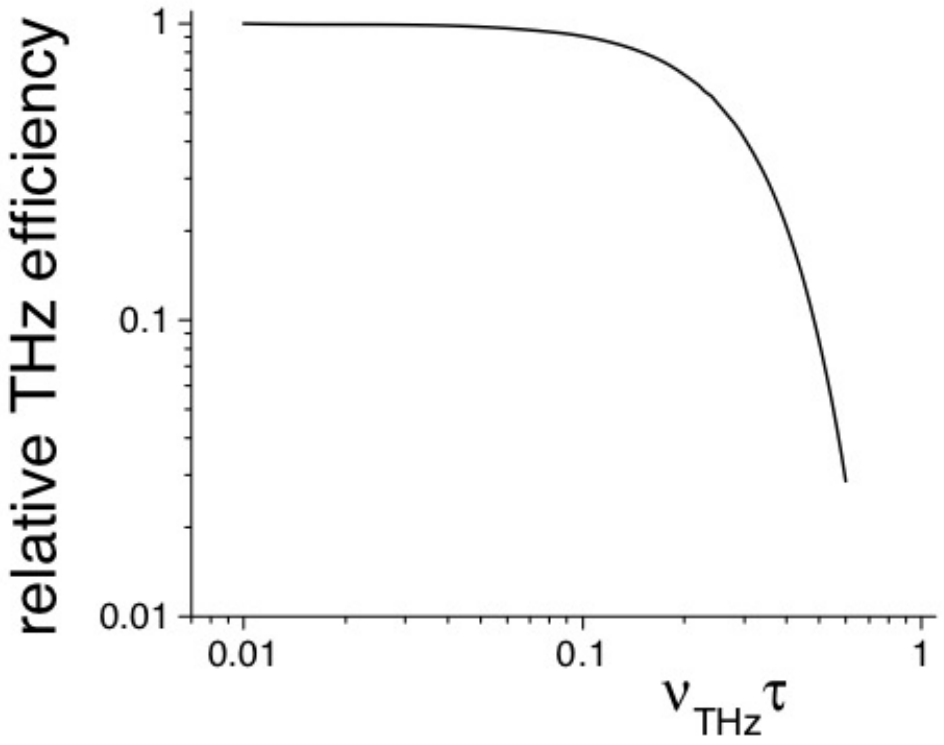


Figure 11.11: Relative THz generation reduction due to $g_1(\Omega_0)$.

# For long pulses

$$\eta_{THz}^{PW,lp} = \frac{\Omega^2\ d_{eff}^{QPM,2} E_o^2 \tau}{2\sqrt{2\pi}c^2\ n_{p,opt} n_{p,THz}} L^2 \int_0^{+\infty} e^{\left(-\frac{\tau^2(\Omega-\Omega_0)^2}{4}\right)}\ \mathrm{sinc}^2\left(\frac{\pi}{2}\frac{\Omega-\Omega_0}{\Delta\Omega}\right) d\Omega, \quad (11.35)$$

$$= \frac{\Omega^2\ d_{eff}^{QPM,2} E_o^2 \tau}{2\sqrt{2\pi}c^2\ n_{p,opt} n_{p,THz}} L^2 \int_0^{+\infty} e^{\left(-\frac{\tau^2(\Omega')^2}{4}\right)}\ \mathrm{sinc}^2\left(\frac{\pi}{2}\frac{\Omega'}{\Delta\Omega}\right) d\Omega'. \quad (11.36)$$

**Walk-off**

$$l_w = \frac{\sqrt{\pi}c\tau}{(n_{g,opt} - n_{p,THz})}$$

$$\eta_{THz}^{PW,lp} = \frac{\Omega^2\ d_{eff}^{QPM,2} E_o^2}{2\sqrt{2\pi}c^2\ n_{p,opt} n_{p,THz}} L^2 \int_0^{+\infty} \exp^{\left(-\frac{y^2}{4}\right)}\ \mathrm{sinc}^2\left(\frac{\sqrt{\pi}}{2}\frac{L}{l_w}y\right) dy,$$

$$\eta_{THz}^{PW,lp} = \frac{\Omega^2\ d_{eff}^{QPM,2} E_o^2}{\sqrt{2}c^2\ n_{p,opt} n_{p,THz}} \frac{l_w L}{\pi} g_2\left(\frac{2l_w}{L}\right)$$

$$g_2(x) = \int_0^{+\infty} \exp\left(-\frac{x^2\mu^2}{\pi}\right)\ \mathrm{sinc}^2(\mu)\ d\mu, \ \text{with}\ x = \frac{2l_w}{L}.$$

# Influence of walk-off

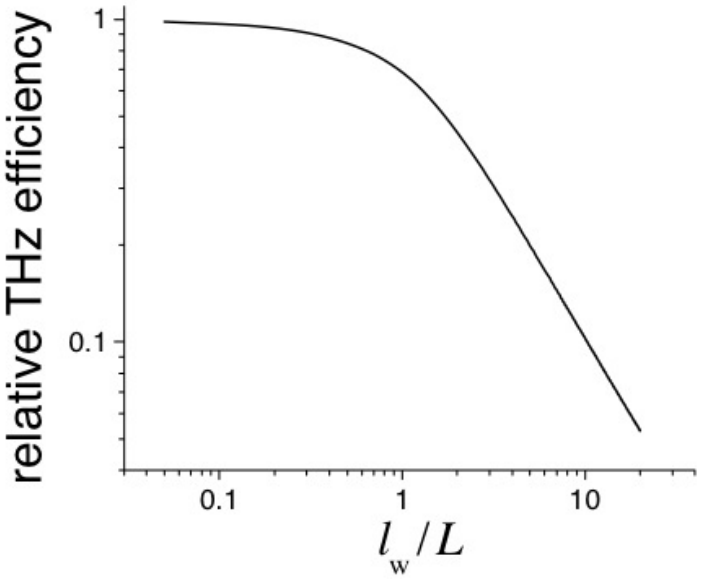


Figure 11.12: Relative THz generation reduction due to $g_2(2\frac{l_w}{L})$.

# Very long pulses

$$\eta_{THz}^{PW,lp\to\infty} = \frac{\Omega^2\ d_{eff}^{QPM,2} E_o^2}{2\sqrt{2\pi}c^2\ n_{p,opt} n_{p,THz}} L^2$$

$$= \frac{\Omega^2\ d_{eff}^{QPM,2}}{\pi\varepsilon_0 c^3\ n_{p,opt}^2 n_{p,THz}} \frac{F_{pump}}{\tau} L^2,$$

# Optimal length of the EO crystal

$$\eta_{THz}(L) \sim \frac{1}{\alpha_{THz}} \left[1 - e^{-\alpha_{THz} L}\right] = L_{eff}$$

$$\eta_{THz}(L) \sim g_3 L, \text{ with } g_3 = \frac{1}{\alpha_{THz} L} \left[1 - e^{-\alpha_{THz} L}\right]$$

For $L = 1/\alpha_{THz}$, $g_3 = 0.63$.

# Optimal focusing

$$\eta_{THz} = \frac{U_{THz}}{U_{pump}} = g_1 \; g_3 \; \frac{2\Omega^2 \; d_{eff}^{QPM,2} L}{\varepsilon_0 \; c^2 \; n_{p,opt}^2 n_{p,THz} \left(n_{g,opt} - n_{p,THz}\right)} \; \frac{U_{pump}}{\pi w^2}$$

$\xi = (\lambda \; L/2\pi n_{THz} w^2)$, where $\lambda$ is the THz wavelength

**Ratio between crystal length and THz Rayleigh range**

# Enhancement factor

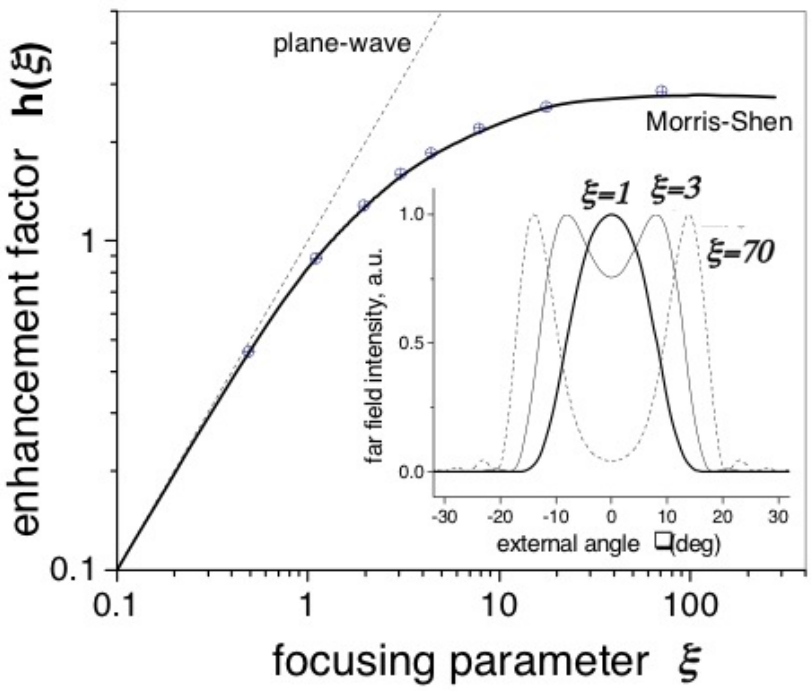


Figure 11.13: Enhancement factor $h$ as a function of the focusing parameter $\xi$. Solid curve is based on Ref. [26]. Dashed curve – plane-wave approximation. Dots represent calculations based on the Green's function method. Inset: far-field THz intensity profiles at different $\xi$ for a 1-cm-long GaAs.

# Cascading and red shift

optical pulse spectrum will be red-shifted by $\Delta\omega/\omega_0 \sim \eta_{THz}$;

$N = 0.5 \times$ (acceptance bandwidth) / (terahertz frequency).

$$\begin{aligned}\frac{d\Delta k}{d\omega} &= \frac{\Omega}{c}\frac{dn_{g,opt}(\omega)}{d\omega} = \frac{\Omega}{c}\frac{dn_{g,opt}(\lambda)}{d\lambda}\frac{d\lambda}{d\omega} \\ &= \frac{\Omega}{c}\frac{dn_{g,opt}(\lambda)}{d\lambda}\frac{\lambda^2}{2\pi c}\end{aligned}$$

$$\frac{d\Delta k}{d\omega} L\Delta\omega_{acc} = 2\pi$$

$$\Delta\omega_{acc} = \frac{2\pi c\omega}{L\Omega}\left(\lambda\frac{dn_{g,opt}(\lambda)}{d\lambda}\right)^{-1}.$$

# Summary

$$FOM_1 = \frac{d_{eff}^2}{n_{p,opt}\alpha_{THz}} \tag{11.45}$$

or

$$FOM_2 = \frac{d_{eff}^2}{n_{p,opt}^2(n_{p,THz} - n_{g,opt})}. \tag{11.46}$$

If the maximum propagation distance is limited by the Kerr effect, the critical FOM becomes

$$FOM_3 = \frac{\lambda_{opt}\ d_{eff}^2}{n_{p,opt}^2 n_{p,THz}\alpha_{THz} n_2}. \tag{11.47}$$